8

Nonlinear Left-Handed Metamaterials

Alexander B. Kozyrev and Daniel W. van der Weide
Department of Electrical and Computer Engineering
University of Wisconsin,
Madison
USA

1. Introduction

Metamaterials are artificial structures that are designed to exhibit specific electromagnetic properties required for different applications but not commonly found in nature. The methodology of synthesizing materials composed of micro- and nano-structured components that mimic the electromagnetic response of individual atoms and molecules (meta-atoms and meta-molecules) has proven to be very productive and resulted in the development of metamaterials exhibiting strong magnetic response at microwave and optical frequencies and so-called left-handed metamaterials (LHMs) (both impossible in conventional real-world materials).

LHMs are designed to exhibit simultaneously negative permittivity and permeability (Veselago, 1968; Engheta & Ziolkowski, 2006). In 2000, Smith et al. developed the first experimental left-handed structure, which was composed of metallic split-ring resonators and thin metal wires (Smith et. al., 2000; Shelby et. al., 2001). An alternative transmission line approach for left-handed materials was proposed, almost simultaneously, by several different groups (Belyantsev & Kozyrev, 2002; Caloz & Itoh, 2002; Iyer & Eleftheriades, 2002). This approach, based on nonresonant components, allows for low-loss left-handed structures with broad bandwidth. The unique electrodynamic properties of these materials, first postulated by Veselago in 1968, include the reversal of Snell's law, the Doppler effect, Vavilov-Cherenkov radiation, and negative refractive index, making theses materials attractive for new types of RF and microwave components. The range of applications for LHMs is extensive, and opportunities abound for development of new and powerful imaging and communication techniques. The most tantalizing of these potential applications is the possibility of realizing "perfect" (diffraction-free) lenses based on their inherent negative index of refraction (Pendry, 2000). The slab of LHM can act as an ideal (diffraction-free) lens and thus capable of producing images of objects without any loss of information which is impossible with conventional lenses.

Most studies of LHMs have been concerned with linear wave propagation, and have inspired many applications that were unthinkable in the past (Engheta & Ziolkowski, 2006; Lai et. al., 2004) such as LH phase shifters (Anioniades & Eleftheriades, 2003), LH directional couplers (Caloz et. al., 2004a; Liu et. al., 2002a), and leaky-wave antennas (Lim et. al., 2005;

Liu et. al., 2002b; Grbic & Eleftheriades, 2002). Materials that combine *nonlinearity* with the anomalous dispersion exhibited by LH media (Lapine & Gorkunov, 2004; Lapine et. al., 2003; Powell et. al., 2007; Shadrivov et.al., 2006), however, give rise to a new class of phenomena and promising applications (Zharov et.al., 2003; Shadrivov & Kivshar, 2005; Shalaev, 2007). Here we present a review of the basic *nonlinear* wave propagation phenomena in LH media. We consider left-handed nonlinear transmission lines (LH NLTL) as the simplest systems that would allow us to combine anomalous dispersion with nonlinearity in a controlled fashion. Understanding the nonlinear phenomena in LH NLTL media is important for both the development of new devices and improvement of the performance of recent tunable devices based on LH NLTLs like phase shifters (Kim et. al., 2005a), tunable leaky-wave antennas (Lai et. al., 2002; Sievenpiper, 2005) and notch filters (Gil et. al., 2004).

2. Comparison of conventional RH and LH nonlinear transmission lines

The transmission line approach proves to be a useful description of LH media. It provides insight into the physical phenomena of LH media and is an efficient design tool for LH applications (Lai et. al., 2004). A LH NLTL is the dual of a conventional nonlinear transmission line shown in Fig. 1*b* where inductors are replaced with capacitors and capacitors with inductors. The effective permeability and permittivity of one-dimensional transmission line metamaterials in the lossless case are expressed as follows:

$$\mu_{eff} = -\frac{2d}{\omega^2 C_L}\ ;\ \varepsilon_{eff} = -\frac{d}{\omega^2 L_L}$$

where d is the period of the LH NLTL and ω is the radian frequency. In contrast with RH NLTL where capacitance gives rise to electric nonlinearity, nonlinear capacitances C_L introduce magnetic-type nonlinearity into the LH NLTL (i.e. effective magnetic permeability becomes nonlinear).

Although both the RH and LH NLTLs use the same components arranged in a similar way, the performance of these two circuits is dramatically different. This difference primarily comes from the difference in their dispersion characteristics (see Fig. 1*c*).

A conventional (right-handed) nonlinear transmission line has normal dispersion and frequency increases with the wavenumber. The fundamental wave can travel synchronously with its higher harmonics. In contrast to the RH NLTL, the LH transmission line exhibits anomalous dispersion and frequency decreases with the wave number (see Fig. 1*c*). The waves propagating in such media are also known as backward waves because the direction of group velocity v_g is opposite to phase velocity ($v_p \cdot v_g < 0$). The fundamental wave can travel synchronously with its higher harmonics. The nonlinearity in RH NLTLs provides energy flow to higher frequencies, which results in waveform sharpening and shock wave formation (Gaponov et. al., 1967; Kataev, 1966). Dispersion, however, results in waveform spreading. If a transmission line exhibits both nonlinearity and dispersion, the latter may compensate the nonlinearity, thus resulting in the formation of temporal solitons (Hirota & Suzuki, 1973).

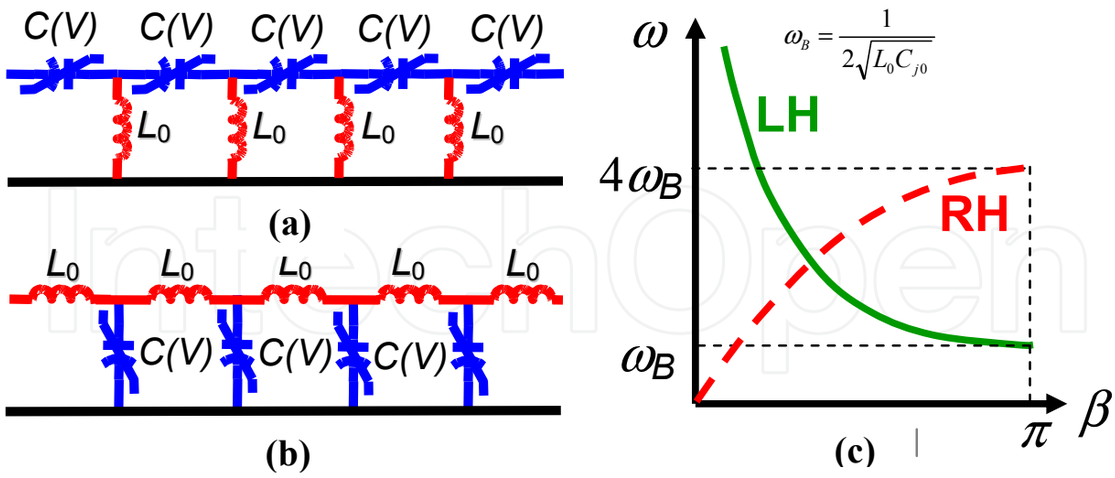

Fig. 1. (a) Equivalent circuit of a LH NLTL; (b) Equivalent circuit of a dual RH NLTL; (c) Typical dispersion curves of LH NLTL (solid line) and RH NLTL (dashed line). Here $\omega_B = 1/(L_0 C_0)^{1/2}$.

Nonlinear transmission lines first drew attention in connection with the idea of distributed parametric amplification. It had been predicted that a distributed parametric amplifier or oscillator circuit could exhibit superior stability of operation and efficiency over lumped parametric circuits (Cullen, 1958; Tien, 1958). Lumped parametric amplifiers were popular as very low-noise alternatives to vacuum tubes prior to the widespread use of semiconductor amplifiers (Louisell, 1960). (Parametric resonance responsible for amplification in lumped circuits is similar to the physical mechanism playing on a swing which allows large amplitudes by alternately raising and lowering the center of mass at a certain relation between the frequency of the swing and the frequency of external force.) Their complexity (they require external resonators and matching circuits) and low efficiencies however made them less attractive for widespread use. Conventional NLTLs were thought to be very promising candidates for use in distributed amplifiers because they do not require external resonant circuits and conversion efficiency was claimed to be very high due to a cumulative effect of parametrically interacting waves propagating along NLTLs.

It turned out that parametric interactions (such as three- and four-wave mixing of phase matched waves) in RH NLTLs typically compete with shock wave formation. For instance, parametric generation and amplification in dispersionless RH transmission lines is entirely suppressed by shock wave formation (Landauer, 1960a; Landauer, 1960b). In contrast to conventional NLTLs, both nonlinearity and dispersion present in LH NLTLs (see Fig. 1) lead to waveform spreading (Caloz et. al., 2004b), consequently making shock wave and electronic soliton formation impossible. Anomalous dispersion makes sharp field transients in left-handed NLTL unstable. Once created, they decompose very quickly during propagation of the waveform due to substantial difference in the phase velocities of the propagating waves. This inability to form shock waves enables a variety of parametric processes to occur instead (Kozyrev et. al., 2005; Kozyrev & van der Weide, 2005a). Furthermore, since the parametric interactions no longer compete with shock wave

formation, it is possible to use stronger nonlinearities, consequently achieving considerable gain in shorter transmission lines (Kozyrev et. al., 2006).

Both theoretical (Kozyrev & van der Weide, 2005a, 2004) and experimental (Kozyrev et. al., 2005, 2006) investigation demonstrate that nonlinear wave form evolution in a LH NLTL can be understood in terms of competition between harmonic generation, subharmonic generation, frequency down conversion and parametric instabilities.

3. Higher harmonic generation

3.1 Theoretical consideration

In short LH NLTLs, harmonic generation dominates over parametric instabilities (Kozyrev et. al., 2005). The amplitude of the second harmonic in the *n*-th section of a LH NLTL $V_2(n)$ can be obtained using a small signal approach described in (Kozyrev & van der Weide, 2005):

$$\left|V_2(n)\right| \approx \frac{4K_N V_1^2(0)\sin^2\left(\frac{\beta_1}{2}\right)\cdot\sin^2(\beta_1)}{\sin\left(\frac{\beta_2}{2}\right)\cdot\left[\sin^2\left(\frac{\beta_2}{2}\right)-\sin^2(\beta_1)\right]}\cdot e^{-\alpha n}\cdot\left|\sin\left[(\beta_2-2\beta_1)n/2\right]\right| \tag{1}$$

where K_N is a "nonlinearity factor" dependent only on diode parameters, $V_1(0)$ is the voltage at the input of the LH NLTL, α is the attenuation constant, *n* is the section number and β_1 and β_2 are the propagation constants (phase shift per section) for the fundamental wave and its second harmonic, respectively.

The fundamental wave propagating in the LH NLTL is always badly mismatched with its higher harmonics due to inherent anomalous dispersion, yet the generation of higher harmonics can still be very effective. This is possible because of "amplitude singularities". The denominator in (1) has zeros when

$$\sin^2(\beta_2/2)-\sin^2(\beta_1)\to 0\,. \tag{2}$$

Due to phase mismatch, the amplitude of the second harmonic varies rapidly with distance. This gives rise to a highly localized energy exchange between the fundamental wave and its second harmonic. It is apparent from (1) that the maximum amplitude of the second harmonic at the end of the *N*-section line is achieved when

$$(\beta_2-2\beta_1)N=(2k+1)\pi\,,\ k=0,1,2,3... \tag{3}$$

The same approach applied to RH NLTL predicts linear growth of the second harmonic amplitude (in the lossless case) due to its phase-matching with fundamental wave (Kozyrev & van der Weide, 2005a; Champlin & Singh, 1986). Thus, the theoretical analysis of 2nd harmonic generation in LH NLTLs shows that, despite the large phase mismatch, inherent anomalous dispersion enables the possibility of faster-than-linear growth of the second harmonic amplitude as predicted by (1) in a narrow frequency range where condition (2) is satisfied. This fact explains the dominance of harmonic generation in short LH NLTLs over

other parametric instabilities which require long distances of propagation for energy exchange to occur because of long coherence distance (due to phase matching). A somewhat similar singular behavior of the second harmonic amplitude was predicted for the wave reflected from a slab of nonlinear LH medium (Agranovich et. al., 2004).

3.2 Experiment

We fabricated a 4-section LH NLTL having identical sections (shown in Fig. 2*a*) (Kozyrev et.al, 2005). The circuit was realized on a Rogers RT/Duroid 3010 board with ε_r = 10.2 and thickness h = 1.27 mm. The nonlinear capacitance in each section is formed by two back-to-back M/A-COM hyperabrupt junction GaAs flip-chip varactor diodes (MA46H120) with DC bias applied between them. Shunt inductances were implemented with 0.12 mm diameter copper wires connecting the pads to the ground plane on the back side of the board. The pads on the board surface, together with inherent parasitics introduce unavoidable series inductance and shunt capacitance, making the whole circuit a composite right/left-handed transmission line having the equivalent circuit shown in Fig. 2*b*. The dispersion characteristic of a composite right/left-handed transmission line has two passbands divided by the stop band. The low frequency passband exhibits anomalous dispersion (left-handed passband) while the high-frequency one is right-handed. Fig. 3 shows the magnitude of the linear wave transmission (S_{21}) of the LH NLTLs. We measured a –6 dB cut-off frequency at 2.7 GHz for 0 V-bias. The frequency region from 2.7 GHz to 8 GHz for 0 V bias corresponds to the left-handed passband. Parameters of the circuit model in Fig. 2*b* were extracted from the *S*-parameters measured at 0 V bias. They are C_L = 0.99 pF, L_L = 1.695 nH, C_R = 0.05 pF, L_R = 0.966 nH.

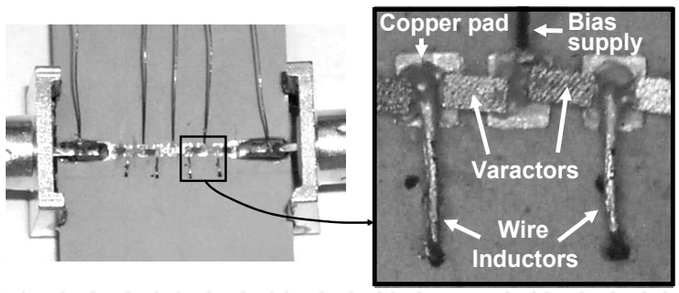

(a)

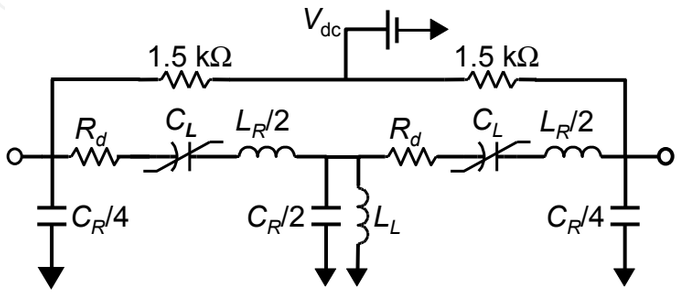

(b)

Fig. 2. (a) Fabricated 4-section LH NLTL and (b) equivalent circuit of one stage.

The measured results qualitatively confirm our predictions using small-signal analysis. Figure 4 shows the spectrum of the waveform from the output of 4-section LH NLTL as measured with an Agilent E4448A Spectrum Analyzer, and corresponds to the maximum of the second harmonic conversion efficiency.

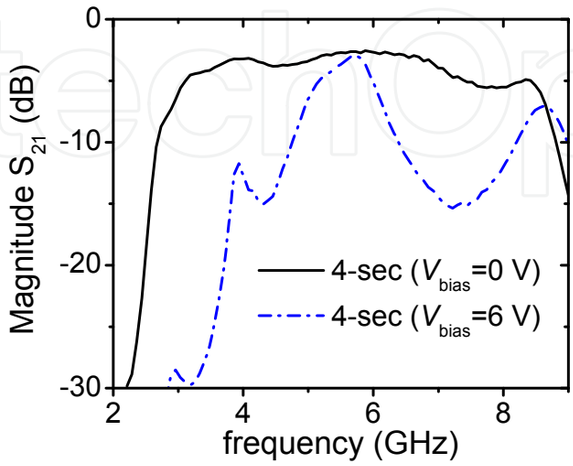

Fig. 3. Measured magnitude of S_{21} parameter for four-section LH NLTL.

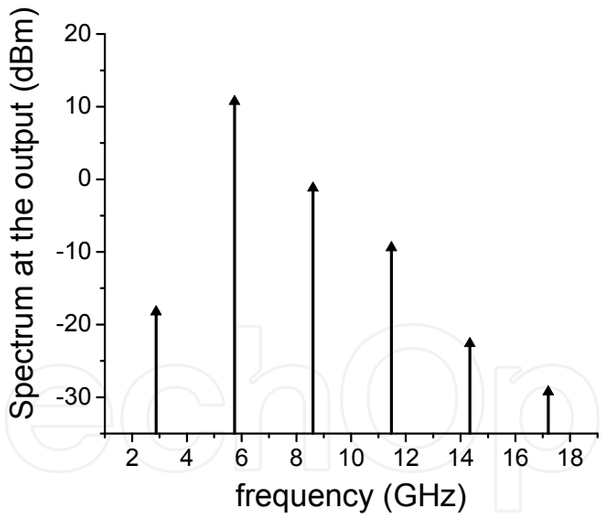

Fig. 4. Spectrum of the output waveform generated by a four-section LH NLTL fed by 2.875 GHz, +17.9 dBm input signal at reverse bias voltage of 6.4 V.

The measured value for the second harmonic conversion efficiency in this 4-section LH NLTL was 19% at 2.875 GHz, using a +17.9 dBm input signal and a reverse bias voltage of 6.4 V. The second harmonic power delivered into a 50 Ω load was +10.72 dBm. The fundamental wave is close to the Bragg cutoff frequency (note the magnitude of S_{21} for the 4-section LH NLTL at bias voltage 6 V as shown in Fig. 2*a*), and thus falls into frequency range for which small-signal analysis predicts amplitude singularity. The second harmonic wave

is close to the transmission maximum, which is located in the middle of the left-handed passband. A fundamental of 2.875 GHz generates numerous higher harmonics, with the second harmonic dominating over the fundamental and the other harmonics. Thus, the LH NLTL combines the properties of both a harmonic generator and a bandpass filter, and under certain conditions may provide an almost pure higher harmonic at its output.

The conversion efficiency observed in the LH NLTL is comparable with the per-stage efficiency of a hybrid Schottky-diode RH NLTL operated in a lower frequency range (Duchamp et. al., 2003).

4. Parametric generation and amplification

4.1 Theory

Under certain circumstances, harmonic generation may compete with different parametric processes, resulting in unstable harmonic generation. Effective parametric interaction in medium exhibiting a second-order nonlinearity generally requires phase matching of three waves. The anomalous dispersion of a LH NLTL system enables effective parametric interactions of the type:

$$f_1 + f_2 = f_3\,,\ \beta_1 - \beta_2 = \beta_3 \tag{4}$$

In the "parametric oscillator configuration", a high-frequency backward pump wave having a frequency f_3 and wavenumber β_3 is excited by the voltage source connected at the input port of a LH NLTL. It generates two other waves having frequencies f_1 and f_2, such that $f_1 < f_2$ and $f_1 + f_2 = f_3$. The wave having frequency f_2 propagates in the opposite direction relative to the pump wave and the wave having frequency f_1 (this is emphasized in (4) with the minus sign). We therefore have a similar situation to backward wave parametric generation (Gorshkov et. al., 1998; Harris, 1966). The backward-propagating parametrically generated wave f_2 enables internal feedback that results in a considerable energy transfer from the pump wave to the parametrically excited waves.

If the amplitude of a high-frequency pump wave exceeds a certain threshold value, it may parametrically generate two other waves. This threshold value depends on the loss present in the LH NLTL, its length and the boundary conditions (matching) at the input and output. No parametric generation occurs when the amplitude of the voltage source is below this value. However, when a weak signal wave is fed into the LH NLTL together with a pump wave having an amplitude below the threshold value, a parametric amplification is observed. In this case, we have two input waves: an intense pump wave and a weak signal wave (Yariv, 1988). The power from the pump wave is transferred to the signal wave, thus amplifying it. A third parasitic idler wave is generated which provides phase matching. From a previous analysis (Gorshkov, et. al. 1998), for the lossless case, the frequencies and powers of these waves also obey the nonlinear Manley-Rowe relations.

4.2 Experiment

Though generation of higher harmonics dominates in short LH NLTLs, in longer transmission lines parametric interactions predominate. We observed efficient parametric

amplification in 7-section LH NLTL (Kozyrev et. al., 2006) shown in Fig. 5. The design of the 7-section LH NLTL is similar to the design of four-section LH NLTL described in the previous section.

However, this time, the series nonlinear capacitance has been implemented with Skyworks Inc. SMV 1233 silicon hyperabrupt varactors and shunt inductances with high-Q 10 nH chip inductors (Murata LQW18A_00).

Fig. 6 shows the magnitude and phase of the linear wave transmission (S_{21}) of this 7-section LH NLTL. Parameters of the circuit model in Fig. 2*b* were extracted from the measured *S*-parameters using Agilent ADS software. They are C_L (3.823 V) = 1.34 pF, L_L = 11.43 nH, C_R = 0.62 pF, L_R = 3.18 nH. The dashed line in Fig. 6 shows the magnitude of S_{21} calculated for the circuit model shown in Fig. 2*b* with component values specified above, and it is in a good agreement with measured data. The circuit model of Fig. 2*b* has also been used to calculate the dispersion curve of the LH transmission line as shown in the inset in Fig. 6. As is evident from *S*-parameters and dispersion curve presented in Fig. 6, the transmission line has a left-handed passband (phase velocity is anti-parallel with the group velocity) from 800 MHz to 1.9 GHz at -3.823 V bias.

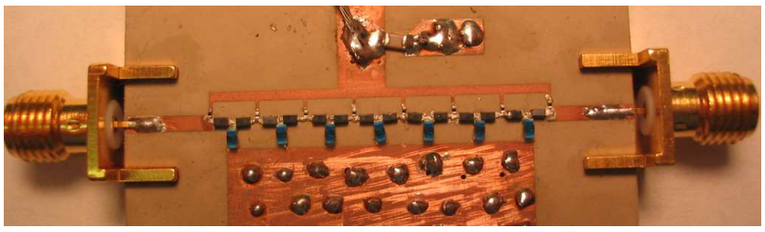

Fig. 5. Fabricated seven-section LH NLTL.

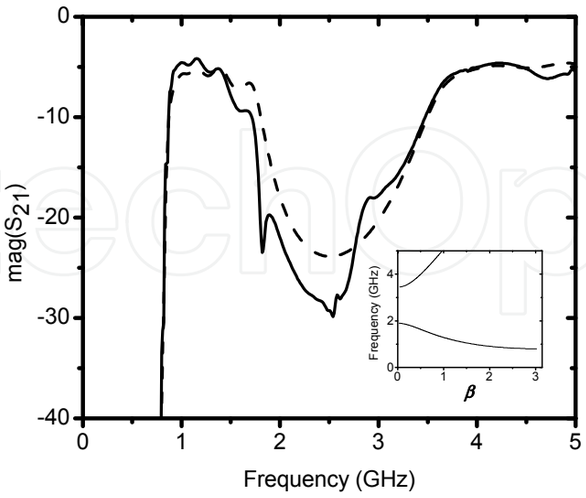

Fig. 6. Measured and simulated (dotted lines) magnitudes of S_{21} parameter for seven-section LH NLTLs for the reverse bias voltage V_B = 3.823 V. Inset shows dispersion curve of the LH NLTL (dependence of the frequency vs relative wave number β).

Figure 7 demonstrates the effect of the intensive pump wave, having frequency $f_p = f_3$, on a weak signal wave ($f_s = f_2$). Figure 7*b* shows the spectrum at the output of the 7-section LH NLTL when only a 1.7279 GHz, 13.96 dBm intensive pump wave is applied at the input. The magnitude of the pump wave was chosen so as to be 0.1 dB below the threshold value required for the occurrence of parametric generation, which manifests itself in distinct, narrow peaks corresponding to the parametrically generated frequencies.

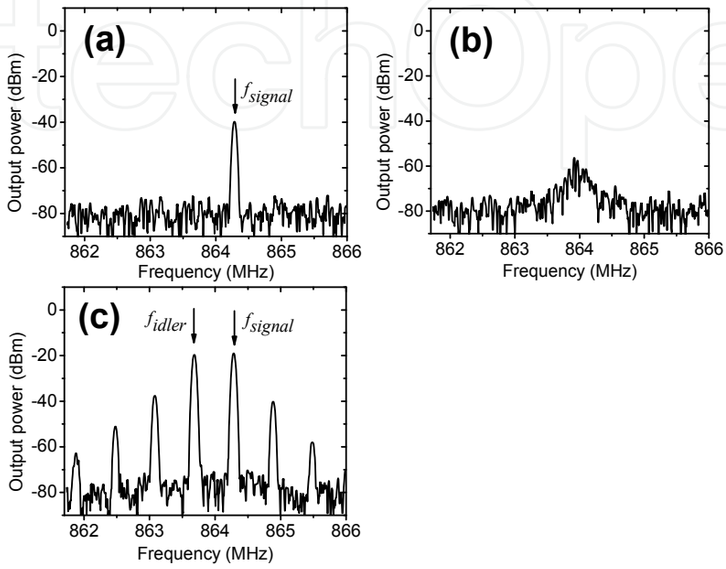

Fig. 7. Spectra of the output waveforms generated by a 7-section LH NLTL fed by: (a) only weak signal source 864.252 MHz, -28 dBm; (b) only pump source 1.7279 GHz, 13.96 dBm; (c) simultaneously signal and pump sources specified in (a) and (b). Reverse bias voltage is 3.87 V.

Figure 7a shows the spectrum at the output when only the 864.252 MHz, -28 dBm signal wave is applied at the LH NLTL input (no pump wave). The graph shows 11.7 dB attenuation of the weak signal wave at the output due loss in the NLTL and power conversion to higher harmonics. And finally, Fig. 7c shows the spectrum at the output when the signal and the pump wave are both applied concurrently at the input of the 7-section LH NLTL. In this spectrum, the components corresponding to the signal wave ($f_s = f_2$), idler wave (f_1), as well as many difference frequencies generated due to the strong nonlinearity in LH NLTL, are evident. Thus, the application of the intensive pump wave results in amplification of the weak signal by 9 dB.

It should be mentioned that parametric amplification of the signal wave propagating in the backward direction with respect to the pump wave has been observed in a round-trip configuration (when both the signal and the pump waves are still applied at the TL input). The parametric interaction of the counter-propagating signal and pump waves becomes possible since both the signal and the pump waves are subject to a strong reflection while propagating along the LH NLTL. This reflection originates from the mismatch at the input and output ports (which is unavoidable due to strong nonlinear variation of capacitance) and results in a standing wave formation. This enables the phase matching of the incident signal wave and the reflected from the output end of the LH NLTL pump wave and hence the parametric interaction of the counterpropagating backward waves.

Figure 8 represents the measured gain of a weak 864.252 MHz signal stimulated by an intense 1.7279 GHz pump wave versus the power of the signal at the input, for fixed values of the pump power. The gain was calculated as the difference between the power of the signal at the output and the power at the input when both are expressed in dBm. Thus, we measured a greater than 10 dB amplification of the signal with power of –32 dBm and below for the power of the pump wave at the input of 13.96 dBm. The measured dependencies of gain verses input signal power becomes flatter with decreasing pump power, thus revealing the potential for amplification in a broad band of the signal power. The results of our measurements in Fig. 8 are in a good agreement with the results of simulations reported in (Kozyrev & van der Weide, 2005b).

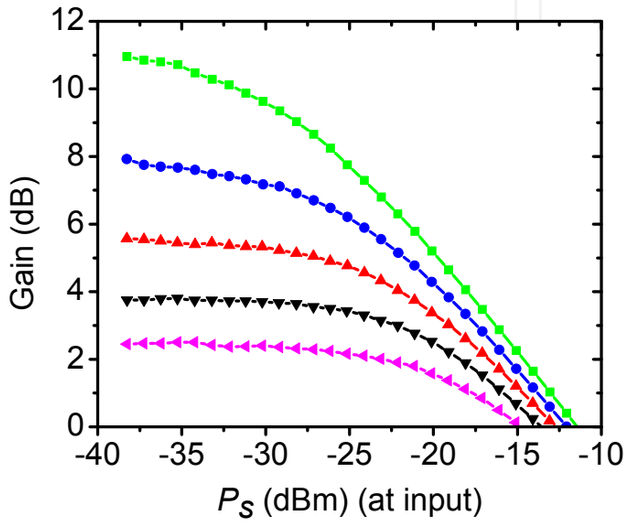

Fig. 8. Measured gain vs power of the signal at the input of LH NLTL for different values of the power of the pump wave at the input $P_{p,in}$.: Green squares - $P_{p,in}$ = 13.96 dBm; Blue circles - $P_{p,in}$ = 13.86 dBm; Red up triangles - $P_{p,in}$ = 13.76 dBm; Black down triangles - $P_{p,in}$ = 13.66 dBm; Magenta left triangles - $P_{p,in}$ = 13.56.

4.3 Higher-order parametric processes

Efficiently generated higher harmonics may also initiate the parametric process. A wave at 2.875 GHz cannot parametrically generate any other waves in the 4-section LH NLTL, shown in Fig. 2, since they would exist below the line's cutoff frequency. The second harmonic at 5.75 GHz excites waves with frequencies of 2.2 GHz and 3.55 GHz depicted in Fig. 9*b* as f_1 and f_2. This basic parametric process then initiates multiple higher-order parametric interactions, resulting in multiple peaks in the spectrum of the output waveform. The progression of this process is shown in Fig. 9*c*, which illustrates conversion of a monochromatic input signal into a wideband output. Further increase in the reverse bias voltage leads to the stabilization of the harmonic generation and suppression of parametric instability (Fig. 9*d*). The variation of bias voltage results in a corresponding change in the dispersion characteristics of the LH NLTL (propagation constants of the interacting waves). This change allows for enabling or disabling of certain nonlinear interactions (phase matching). In our particular case it enables/disables higher-order parametric interactions.

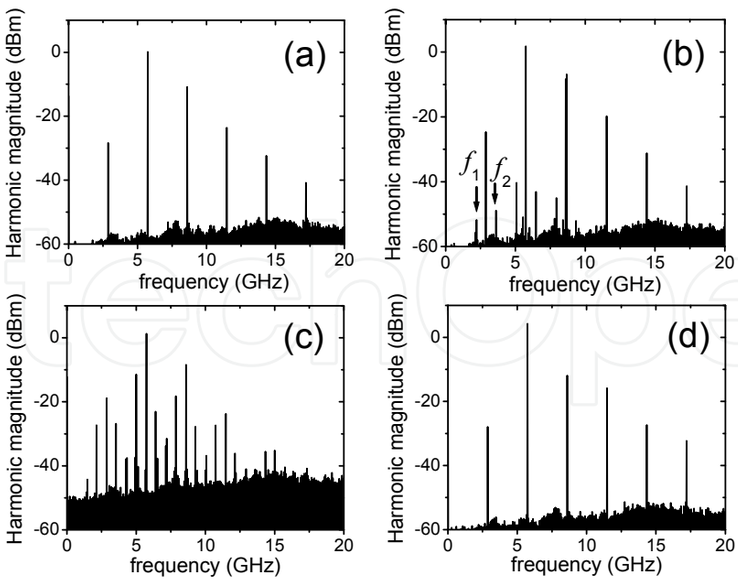

Fig. 9. Spectra of the output waveform generated by a 4-section LH NLTL fed by 2.875 GHz, +19 dBm input signal for different values of the bias voltage (*a* – 4 V, *b* – 4.95 V, *c* – 5 V, *d* – 6.3 V). The results here are decreased by 6 dB due to a protection attenuator.

4.4 Higher-order parametric processes

Parametric amplification can be of interest for building "active" or "amplifying" metamaterials and for providing a means to compensate for inherent LH media loss, a challenge for currently existing metamaterials (Kozyrev et. al., 2006). The primary drawback of current negative-index metamaterials (NIMs) (for example those composed of the arays of metallic wires and split-ring resonators) is their considerable loss, which renders the results ambiguous and the materials all but useless for practical applications. These losses have been overcome to some extent by careful fabrication and assembly techniques (Houck et. al. 2003), but still remain the primary obstacle to using NIMs in imaging applications. It was shown (Tretyakov, 2001) that due to causality requirements, the use of conventional composite NIMs (based on arrays of metallic wires and arrays of split-ring resonators) does not allow for the realization of low-loss NIMs without the incorporation of some active components (transistor amplifiers, etc.) in a composite NIM. The idea of using parametric amplification to compensate for inherent loss in optical left-handed systems has been also discussed in (Popov & Shalaev, 2006).

5. Envelope solitons in LH NLTLs

Besides the nonlinear evolution of a waveform itself, another class of phenomena involving evolution of amplitude and phase of continuous waves is also possible. This type of nonlinear wave propagation phenomena arise in NLTLs having strong frequency dispersion with respect to the average amplitude for amplitude-modulated wave containing a carrier of relatively high frequency and slow (optical-type) nonlinearity. This dispersion may lead to amplitude instability as well as to formation of envelope solitons and periodic modulation of a carrier wave propagating in a stationary manner. The observation of amplitude

instability and envelope soliton generation in conventional (RH) NLTLs has already been the subject of many publications (Lonngren & Scott, 1978; Ostrovskii & Soustov, 1972; Yagi & Noguchi, 1976). The experimental observation of the generation of the trains of envelope solitons in LH NLTLs arising from the self-modulational instability under certain conditions of the amplitude and frequency of the pump wave was first reported in (Kozyrev & van der Weide, 2007).

The analysis of LH NLTLs is straightforward when the equations governing envelope evolution can be reduced to the one-dimensional cubic nonlinear Schrodinger equation (NSE), which provides a canonical description for the envelope dynamics of a quasi-monochromatic plane wave (the carrier) propagating in a weakly nonlinear dispersive medium when dissipative processes (including nonlinear damping due to higher harmonic generation and nonlinear wave mixing) are negligible (Gupta & Caloz, 2007; Narahara et. al., 2007). However, in most of the practical situations the parametric decay instabilities and higher harmonic generation can be very significant (Kozyrev et. al, 2005, 2006; Gorshkov et. al., 1998; Lighthill, 1965). The threshold for parametric generation is known to be very low (lower then in conventional RH NLTLs). In order to realize the scenario described by the NSE, the LH NLTL should be operated below this threshold so that the nonlinearity should be very weak and the NLTL impractically long. In contrast, we performed an experimental study of nonlinear envelope evolution and envelope soliton generation in relatively short LH NLTLs and when nonlinear damping is very strong. We are also taking advantage of a fast nonlinearity introduced by Schottky diodes when nonlinear capacitance is a function of the instantaneous value of voltage along the line rather then its amplitude, a type of nonlinearity not described in the framework of the NSE and its modifications developed for slow (retarding) nonlinearity.

Figure 10 shows a typical voltage waveform and its spectrum measured at the output of 7-section LH NLTL in the envelope soliton generation regime. This voltage waveform is a cw signal with carrier at fundamental (pump) frequency and with an envelope representing itself a train of bright solitons appearing as periodic pulses above a cw background. The scenario of the development of modulational instability and/or generation of envelope solitons is very sensitive to the parameters of the signal applied at the input of NLTL. Depending on the amplitude and frequency of the input signal, trains of envelope solitons of different shape and types can be generated. Figure 11 shows envelopes of the measured waveforms at the output of 7-section LH NLTL. These envelopes' functions have been obtained by applying the Hilbert transform to the original voltage waveforms.

Traces (a), (b) and (c) in Fig. 11 show trains of bright envelope solitons of different shapes while traces (d) and (e) show periodic trains of so-called dark solitons (dips in the cw background). The trains of envelope solitons that we observed are also known as cnoidal waves. The interval between individual solitons depends on the amplitude and frequency of the input signal but does not depend on the length of LH NLTL. Comparison of voltage waveforms at the output of 7-, 10- and 17-section LH NLTL for the same input signal parameters shows that the distance between solitons and their shape are preserved during propagation along transmission line and that we deal with the generation of stationary train of solitons. The envelope shape is not smooth since strong nonlinearity gives rise to numerous higher harmonics and subharmonics of carrier frequency. In the spectral domain, generation of envelope solitons manifests itself in the appearance of spectral regions with

numerous closely spaced spectral harmonics. The interval between adjacent spectral components is $\Delta f = 1/\tau$, where τ is the period of the train of solitons.

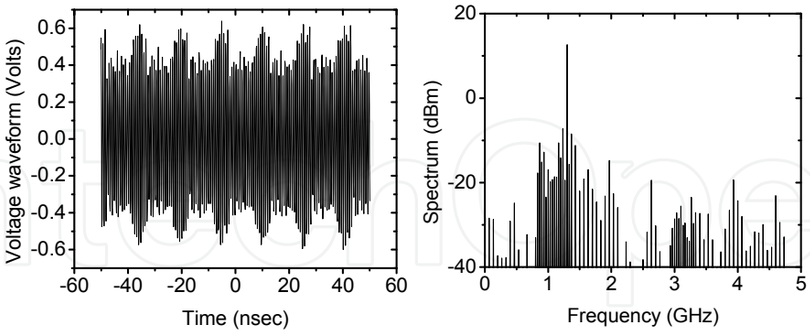

Fig. 10. Voltage waveform (a) and its spectrum (b) measured at the output of 7-section LH NLTL fed by a 1.3125 GHz, +21.6 dBm input signal.

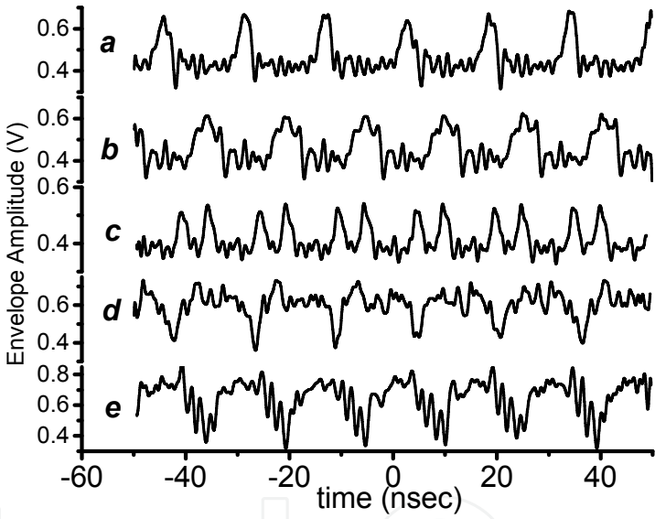

Fig. 11. Measured trains of envelope solitons for different power P_{inp} and the frequency f_{inp} of the input signal. a) f_{inp} = 1.3723 GHz, P_{inp} = 24.66 dBm; b) f_{inp} = 1.3125 GHz, P_{inp} = 21.60 dBm; c) f_{inp} = 1.321596 GHz, P_{inp} = 19.34 dBm; d) f_{inp} = 1.2974 GHz, P_{inp} = 24.64 dBm; e) f_{inp} = 1.102 GHz, P_{inp} = 23.62 dBm

A small variation of the parameters of the input signal leads to switching between the generation of bright and dark solitons [compare traces (a) and (b)] in contrast to the scenario described by the NSE. As is known, systems described by the NSE can be characterized by two main parameters: the nonlinearity parameter $N = \partial\omega/\partial|A|^2$ (ω and A are the carrier frequency and the amplitude) and the dispersion parameter $D = \partial^2\omega/\partial k^2$ (k is the wave number). According to the Lighthill criterion (Lighthill, 1965), either dark or bright solitons are observed depending on the sign of these two parameters. Bright solitons exist when DN<0 and dark solitons exits when DN>0. The observed switching is enabled by the

counterplay of the significant nonlinear damping (due to strong and fast nonlinearity) and strong spatial dispersion exhibited by the periodic LH NLTLs. Neither is taken into account by standard NSE yet both are known to lead to co-existence of bright and dark solitons in other physical systems (Kivshar et. al., 1994; Scott et.al., 2005). For example, somewhat similar processes have recently been observed in the system of an in-plane magnetized single crystal yttrium-iron-garnet (YIG) film in the magnetostatic backward volume wave configuration. However, there is a fundamental issue that distinguishes our work from (Scott et.al., 2005) where the soliton trains have been generated through the nonlinear mode beating of two copropagating magnetostatic backward volume wave excitations in thin YIG film. Thus, a pre-modulated signal was used to achieve soliton generation. In contrast to this work, we applied non-modulated sine wave at the input.

6. Pulse formation in LH NLTL media

As it has already been mentioned in Section 2, both the nonlinearity and dispersion present in LH NLTLs lead to waveform spreading, consequently making shock wave and electronic soliton formation impossible, making them at first blush useless for pulse forming applications. However, this inability to form shock waves enables a variety of parametric processes leading to amplitude istabilitity as well as formation of envelope solitons and periodic modulation of a carrier wave (Kozyrev & van der Weide, 2007) as discussed in the previous section. Here we describe another type of envelope evolution resulting in generation of RF pulses of limited duration with stable amplitude and very short rise/fall times (sharp transients). This type of envelope evolution is primarily enabled by the amplitude-dependent higher harmonic generation rather than self-modulation instability leading to generation of the envelope solitons (Kozyrev & van der Weide, 2010).

Fig. 12 shows a typical dependence of the magnitude of the second harmonics at the output of 7-section LH NLTL shown in Fig. 5 vs magnitude of the input sinusoidal signal. This dependence has three distinct regions. In the first region the power of the generated second harmonic follows a square law as predicted by the small signal analysis (1). When the power of the fundamental wave reaches certain threshold level the second harmonic power jumps by almost 5 dB indicating a bifurcation (multistability region) followed by the saturation region where second harmonic amplitude changes insignificantly with the input power. Step-like dependence of the second harmonic power indicates a bifurcation-type change in the field distribution along the line and formation of field patterns that change dispersion properties of the line resulting in significant increase of the generation efficiency. These field patterns (nonlinear mode build-up) result from the nonlinear interactions and reflection of both fundamental and second harmonic signals from input and output interfaces. An example of such patterns has been investigated in (Kozyrev & van der Weide, 2005a; Kozyrev et. al., 2005) where a significant increase of the 3rd harmonic generation efficiency correlated with self-induced periodicity of the voltage oscillations across nonlinear capacitances on LH NLTL. This self-induced periodicity of the voltage amplitude cross the nonlinear capacitors leads to periodic variation of the capacitance along the line. Due to strong nonlinearity (large capacitance ratio), this periodicity results in a considerable change of the dispersion characteristics and enables quasi-phase matching of the fundamental wave and its higher harmonics.

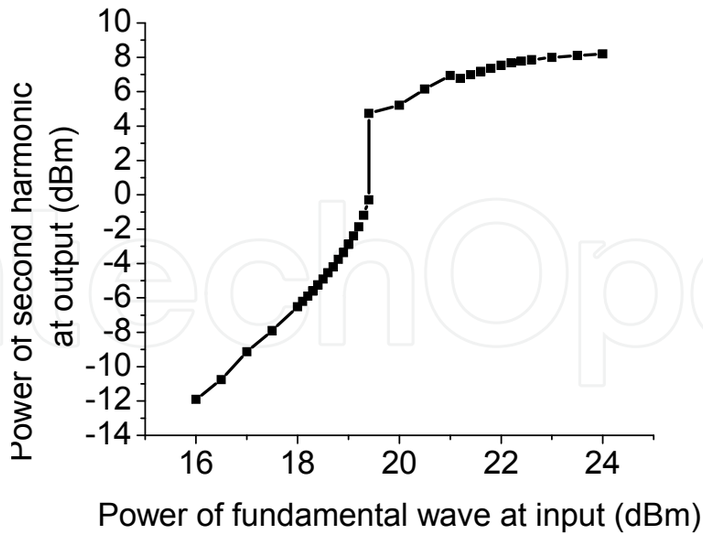

Fig. 12. Dependence of the power of the 2nd harmonic at the output on the power of the fundamental signal at the input in 7-section LH NLTL shown in Fig. 5 measured at 783 MHz and the reverse bias voltage V_B = - 4.1 V.

The step-like dependence of the second harmonic power on the power of the fundamental signal may impact significantly the output waveform if the amplitude in the fundamental wave is modulated around the threshold value. To verify this assumption the LH NLTL was fed by a 783 MHz, +20.5 dBm sinusoidal signal modulated at 100 kHz with the depth of modulation of 50 %. Power of the input signal corresponds to the threshold value in Fig. 12. Figure 13 shows voltage waveforms at the input and output port and spectrum at the output of 7-section LH NLTL. As expected, the voltage waveform at the input is a sinusoidal wave modulated by another sinusoidal signal at 100 MHz. The envelope of the output waveform is dramatically different from the one of the input wave. It represents itself a series of pulses with the shape approaching a rectangular. Furthermore, the carrier frequency of the output signal is the second harmonic of the fundamental signal as revealed by the spectrum presented in Fig. 13*c*. Modulated signal switches second harmonic generation on and off thus enabling generation of a train of RF pulses at the output. Since the fundamental frequency is chosen below the cut-off frequency, it is heavily attenuated in transmission line and only second harmonic is present at the output. Some asymmetry of the shape of the RF pulses at the output is related to the existence of hysteresis and narrow multistability region. The experimental results presented in Fig. 13 clearly demonstrate that a small modulation signal can be used to control the shape, duration and repetition rate of the RF pulses at the output which is very promising to numerous applications.

Our experimental results correlate very well with speculations in (Agranovich et. al., 2004) where authors predicted that the shape of pulses at the output of LH media can be drastically different from those expected from an ordinary nonlinear medium.

Potential applications may include pulse forming circuits, amplifiers of digital signals as well as very efficient modulators at power levels or in frequency ranges not attainable by conventional semiconductor devices.

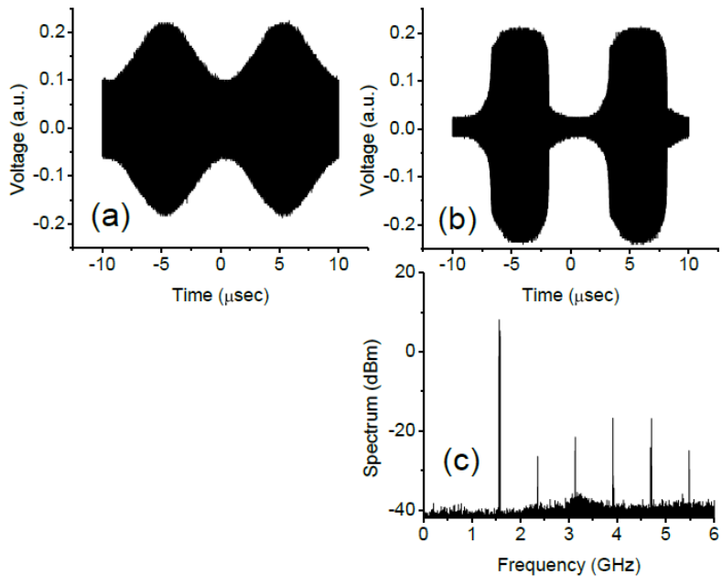

Fig. 13. Voltage waveforms at the input (a) and output (b) port and spectrum at the output (c) of 7-section LH NLTL. Voltage was measured at the coupled output of directional couplers connected at the input and output ports of NLTL.

7. Inverse Doppler effect in nonlinear transmission lines

Some interesting phenomena arise in nonlinear periodic systems (periodically loaded nonlinear transmission lines) supporting propagation of backward spatial harmonics. It is well known that the periodic systems support propagation of the Bloch waves which can be expanded into an infinite set of spatial harmonics (Collin, 1992) so that the field in a periodic structure can be represented as

$$V_B = \sum_{n=-\infty}^{n=\infty} V_{p,n} e^{-j\beta_n z}$$

Each term in this expansion is a spatial harmonic, is periodic in space amplitude

$$V_{p,n}(z+d) = V_{p,n}(z)$$

and has propagation phase constant

$$\beta_n = \beta + 2n\pi / d\,.$$

All harmonics propagate with the same group velocity; however, some of the spatial harmonics have phase and group velocities that are oppositely directed (backward spatial harmonics) since β_n can be both positive and negative and thus exhibit anomalous dispersion:

$$v_g^{(n)} = d\frac{\omega}{\beta_n} \quad v_p^{(n)} = d\frac{\partial\omega}{\partial\beta_n} = d\frac{\partial\omega}{\partial\beta}\,.$$

The first experimental observation of an inverse Doppler effect, in which the frequency of a wave is increased upon reflection from a receding boundary, was reported in (Seddon & Bearpark, 2003). They used an experimental scheme based on a magnetic nonlinear transmission line which was suggested recently in (Belyantsev & Kozyrev, 2002, 1999). This scheme falls into a general class of systems that involve the emission of phase matched high-frequency waves by an electromagnetic shock wave propagating along a NLTL with dispersion (Belyantsev et. al., 1995; Belyantsev & Kozyrev, 1998, 2000). The moving boundary that is used to produce a Doppler shift is the discontinuity that is formed between regions of unsaturated and saturated nonlinearity in the transmission line at the leading edge of the pump pulse. Under appropriate conditions, this shock wave (moving discontinuity) generates a Bloch wave propagating in the opposite direction to the moving discontinuity. It occurs when this shock wave is phase matched with a backward spatial harmonic of the exited Bloch wave. Following its reflection from the NLTL input interface, the excited Bloch wave catches up with the moving discontinuity and produces an anomalous Doppler shift (Belyantsev & Kozyrev, 2002). The detailed theory of this phenomenon is presented in (Kozyrev & van der Weide, 2005, 2006).

8. Nonlinear volumetric metamaterials

Nonlinear phenomena similar to ones described in Sections 3-7 have also been observed in volumetric metamaterials (Shadrivov et. al., 2008a, 2008b). For instance, the selective generation of higher harmonics has been observed in metamaterials consisting of split-ring resonantors (SRR) and metal wires shown in Fig. 14. Each SRR contains a variable capacity diode (model Skyworks SMV-1405) which introduces nonlinear current-voltage dependence and resulting nonlinear magnetic dipole moment to each SRR (Shadrivov et. al., 2008a). In terms of effective medium parameters, the manufactured structure has nonlinear magnetization and non- linear effective magnetic permittivity.

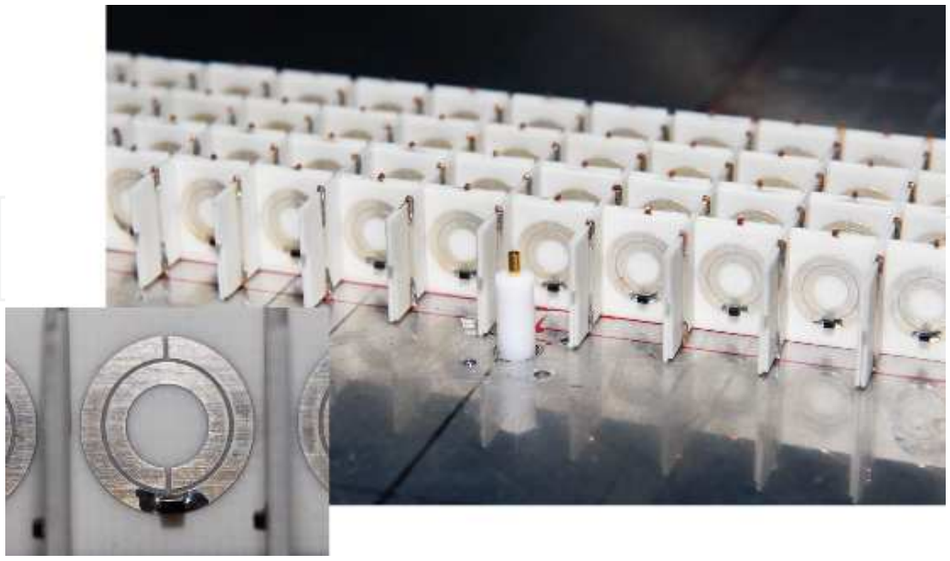

Fig. 14. Photograph of the nonlinear tunable metamaterial created by square arrays of wires and nonlinear SRRs. Each SRR contains a varactor (see the inset) which provides power-dependent nonlinear response.

Arrays of SRRs and wires form a square lattice with 29 x 4 x 1 unit cells of the size of 10.5 mm.

To measure the em field scattering on our samples, the metamaterial slab is placed in a parallel plate waveguide. The planes of SRRs are aligned perpendicular to the parallel plate surfaces. We have measured the spectrum of the transmitted signal for different frequencies of the incident em wave. For this purpose, the input antenna (placed at the midpoint of the lower plate, 2 mm from the metamaterial slab, in front of the central unit cell) was fed by the signal generated by an Agilent E4428C ESG vector signal generator and amplified by a 38 dB amplifier. The signal detected by the receiving antenna placed 2 cm behind the metamaterial slab was analyzed using an Agilent E4448A PSA series spectrum analyzer.

Figure 15 shows spectra of the signal detected by the receiving antenna behind the nonlinear LHM slab. Varying the input frequency, we observed efficient selective harmonic generation. Namely, second (Fig. 15*a*), third (Fig. 15*b*), and fourth (Fig. 15*c*) harmonics were selectively generated. Moreover, the generation of a comblike signal was also observed (Fig. 15*d*).

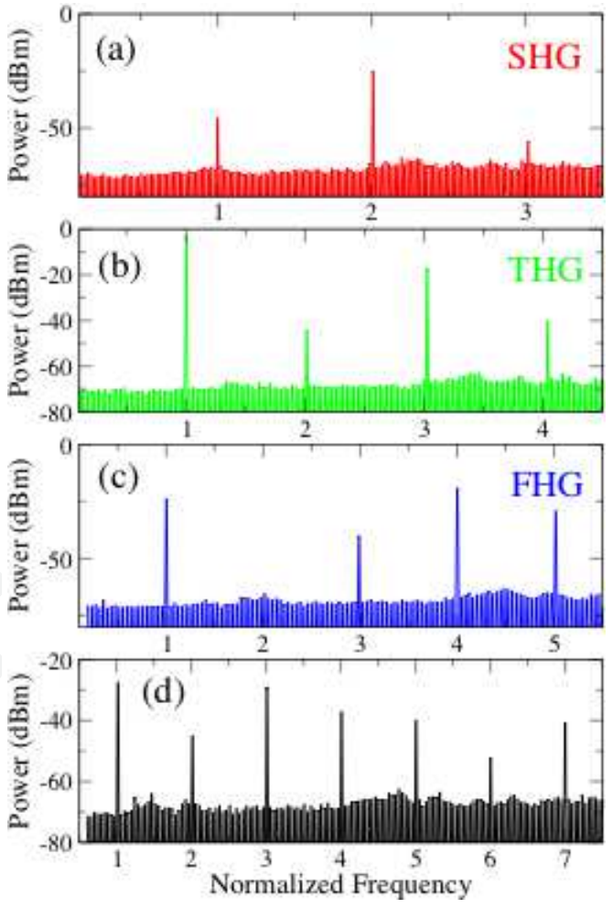

Fig. 15. Spectra of the signals detected by the receiving antenna located behind the nonlinear LHM slab for different source frequencies: (a) 3.415 GHz, (b) 2.29 GHz, (c) 1.733 GHz, and (d) 1.668 GHz. The frequency on each graph is normalized to the corresponding source frequency. Power at the input antenna is +30 dBm.

Selective generation of higher harmonics observed in our experiments is related to the transmission properties of the metamaterial. A particular harmonics dominates over fundamental harmonic and the other higher harmonics when its frequency corresponds to the transparency band. Results of the transmission coefficient measurements performed on our nonlinear LHMs indicate a right-handed transparency band with a maximum transparency at around 7 GHz. This value agrees well with the values of the higher harmonics dominating in our measurements. Furthermore, the presence of very high order harmonics in the spectrum of the trans- mitted signal manifests strong nonlinearity inside the metamaterial which potentially may lead to significant enhancement in nonlinear processes in artificial metamaterials as compared to conventional materials.

9. Conclusion

We have reviewed several nonlinear wave phenomena in LH media, including harmonic generation, parametric amplification and generation of traveling waves, generation of the train of envelope solitons and their competition. Furthermore, LH NLTLs which were considered as a model system in this paper, can be also of interest from the design perspective for development of various compact and robust applications for wireless communications and imaging. LH NLTLs have already been used as the key counterparts of recently designed and implemented tunable phase-shifters, tunable band-pass filters, and the arbitrary waveform generator based on fourier decomposition (by combining broadband power divider, LPF, BPF, HPF, harmonic generator, vector modulator and broadband LNAs on copper board) (Kim et. al., 2005a, 2005b, 2006, 2007). Moreover, extending the results for 1-D LH NLTL to higher dimensions would enable combining harmonic generation in LH NLTL media with focusing (Grbic & Eleftheriades, 2003, 2004), due to the negative refractive index of 2-D or 3-D LH transmission line media. This may lead to the development of highly efficient and powerful frequency multipliers, as well as to building “active” or “amplifying” super lenses. Furthermore, our approach can be also scaled from its current microwave form into terahertz, infrared, and, ultimately, visible form (Goussetis et. al., 2005; Qin et. al., 2007, 2008).

10. Acknowledgment

This work was supported under the Air Force Office of Scientific Research, MURI Grant No F49620-03-1-0420, ‘Nanoprobe Tools for Molecular Spectroscopy and Control’.

11. References

Agranovich, V. M.; Shen, Y. R.; Baughman, R. H. & Zakhidov, A. A. (2004). *Physical Review B* Vol.69, p. 165112.

Anioniades, M. & Eleftheriades G. V. (2003). *IEEE Antennas and Wireless Propagation Letters,* Vol.2, p. 103.

Belyantsev, A. M.; Dubnev, A. I.; Klimin, S. L.; Kobelev, Y. A. & Ostrovskii, L. A. (1995). *Technical Physics,* Vol.40, p. 820.

Belyantsev, A. M. & Kozyrev, A. B. (1998). *Technical Physics,* Vol.43, p. 80.

Belyantsev, A. M. & Kozyrev, A. B. (1999). *Materials Science Forum,* Vol.297, p. 349.

Belyantsev, A. M. & Kozyrev, A. B. (2000). *Technical Physics,* Vol.45, p. 747.

Belyantsev, A. M. & A. B. Kozyrev, A. B. (2002). *Technical Physics,* Vol.47, p. 1477.
Caloz, C. & Itoh, T. (2002). *IEEE Antennas and Propagation Society International Symposium Dig.,* Vol.2, p. 412.
Caloz, C.; Sanada, A. & Itoh, T. (2004). *IEEE Transactions on Microwave Theory and Techniques,* Vol.52, p. 980.
Caloz, C.; Lin, I. H. & Itoh ,T. (2004). *Microwave and Optical Technology Letters,*Vol.40, p. 471.
Champlin, K. S. & Singh, D. R. (1986). *IEEE Transactions on Microwave Theory and Techniques,* Vol.MTT-34, p. 351.
Collin, R. E. (1992). *Foundations for microwave engineering*, 2nd ed.: McGraw-Hill, Inc.
Cullen, A. L. (1958). *Nature,* Vol.181, p. 332.
Duchamp, J.-M.; Ferrari, P.; Fernandez, M.; Jrad, A.; Melique, X.; Tao, J.; Arscott, S.; Lippens, D. & Harrison, R. G. (2003). *IEEE Transactions on Microwave Theory and Techniques,* Vol.51, p. 1105.
Engheta, N. & Ziolkowski, R. W. (2006). *Matamaterials: Physics and Engineering Explorations*: John Wiley & Sonc, Inc.
Gaponov, A. V.; Ostrovskii, L. A. & Freidman, G. I. (1967). *Radiophysics and quantum electronics,* Vol.10, p. 772.
Gil, I.; Garcia-Garcia, J.; Bonache, J.; Martin, F.; Sorolla, M. & Marques, R. (2004) *Electronics Letters,* Vol.40, p. 1347.
Gorshkov, A. S.; Lyakhov, G. A.; Voliak, K. I. & Yarovoi, L. A. (1998). *Physica D,* Vol.122, p. 161.
Goussetis, G.; Feresidis, A. P.; Wang, S.; Guo, Y. & Vardaxoglou, J. C. (2005). *Journal of Optics A: Pure and Applied Optics,* Vol.7**,** p. S44.
Grbic, A. & Eleftheriades, G. V. (2002). *Journal of Applied Physics,* Vol.92, p. 5930.
Grbic, A. & Eleftheriades, G. V. (2003). *Antennas and Wireless Propagation Letters*, Vol.2, p. 186.
Grbic, A. & Eleftheriades, G. V. (2004). *Physical Review Letters*, Vol.92, p. 117403.
Gupta, S. & Caloz, C. (2007). Dark and Bright Solitons in Left-Handed Nonlinear Transmission Line Metamaterials, *IEEE/MTT-S International Symp.*, pp. 979-982.
Harris, S. E. (1966). *Applied Physics Letters,* Vol.9, p. 114.
Hirota, R. & Suzuki, K. (1973). *Proceedings of the IEEE,* Vol.61, p. 1483.
Houck, A. A.; Brock, J. B. & Chuang, I. L. (2003). *Physical Review Letters,* Vol.90, p. 137401.
Iyer, A. K. & Eleftheriades, G. V. (2002). *IEEE MTT-S Int Symp. Dig.,* p. 1067.
Kataev, I. G. (1966). *Electromagnetic Shock Waves*. London: Illife.
Kim, H.; Kozyrev, A. B. & van der Weide, D. W. (2005). *IEEE Microwave and Wireless Components Letters,* Vol.15, p. 366.
Kim, H.; Kozyrev, A. B.; Ho, S.-J. & van der Weide, D. W. (2005). *Microwave Symposium Diges*. p. 4.
Kim, H.; Ho, S. J.; Choi, M. K.; Kozyrev, A. B. & van der Weide, D. W. (2006). *IEEE Transactions on Microwave Theory and Techniques,* Vol.54, p. 4178.
Kim, H.; Kozyrev, A. B.; Karbassi, A. & van der Weide, D. W. (2007). *IEEE Transactions on Microwave Theory and Techniques,* Vol.55, pp. 571-578.
Kivshar, Y. S.; Krolikowski, W. & Chubykalo, O. A. (1994). *Physical Review E,* Vol.50, pp. 5020-32.
Kozyrev, A. B. & van der Weide, D. (2004). *IEEE MTT-S Int. Microwave Symp. Dig.*

Kozyrev, A. B.; Kim, H.; Karbassi, A. & van der Weide, D. W. (2005). *Applied Physics Letters,* Vol.87, p. 121109.
Kozyrev, A. B. & van der Weide, D. W. (2005). *IEEE Transactions on Microwave Theory and Techniques,* Vol.53, p. 238.
Kozyrev, A. B. & van der Weide, D. W. (2005). *IEEE Antennas and Propagation Society International Symposium Dig. P.* 672.
Kozyrev, A. B. & van der Weide, D. W. (2005). *Physical Review Letters,* Vol.94, p. 03902.
Kozyrev, A. B. & van der Weide, D. W. (2006). *Physical Review Letters,* Vol.96, p. 069403.
Kozyrev, A. B.; Kim, H. & van der Weide, D. W. (2006). *Applied Physics Letters,* Vol.88, p. 264101.
Kozyrev, A. B. & van der Weide, D. W. (2007). *Applied Physics Letters,* Vol.91, p. 254111.
Kozyrev, A. B. & van der Weide, D. W. (2010). *Applied Physics Letters,* Vol.96, p. 104106.
Lai, A.; Caloz, C. & Itoh, T. (2004). *IEEE Microwave Magazine,* Vol.5, p. 34.
Landauer, R. (1960). *IBM Journal,* Vol.4, p. 391.
Landauer, R. (1960). *Journal of Applied Physics,* Vol.31, p. 479.
Lapine, M.; Gorkunov, M. & Ringhofer, K. H. (2003). *Physical Review E* Vol.67, p. 065601.
Lapine, M. & Gorkunov, M. (2004). *Physical Review E,* Vol.70, p. 066601.
Lighthill, M. J. (1965). *Journal of the Institute of Mathematics and Its Applications,* Vol.1, p. 269.
Lim, S.; Caloz, C. & Itoh, T. (2005). *IEEE Transactions on Microwave Theory and Techniques,* Vol.53, p. 161.
Liu, L.; Caloz, C.; Chang, C.-C. & Itoh, T. (2002). *Journal of Applied Physics,* Vol.92, p. 5560.
Liu, L.; Caloz, C. & Itoh, T. (2002). *Electronics Letters,* Vol.38, p. 1414.
Lonngren, K. E. & Scott, A. (1978). *Solitons in Action*. New York: Academic Press.
Louisell, W. H. (1960). *Coupled mode and parametric electronics*. New York, London: John
Narahara, K.; Nakamichi, T.; Suemitsu, T.; Otsuji, T. & Sano, E. (2007). *Journal of Applied Physics,* Vol.102, p. 024501.
Ostrovskii, L. A. & Soustov, L. V. (1972). *Izvestiya Vysshikh Uchebnykh Zavedenii, Radiofizika,* Vol.15, p. 242.
Pendry, J. B. (2000). *Physical Review Letters,* Vol.85, p. 3966.
Popov, A. K. & Shalaev, V. M. (2006). *Optics Letters,* Vol.31, p. 2169.
Powell, D. A.; Shadrivov, I. V.; Kivshar, Y. S. & Gorkunov, M. V. (2007). *Applied Physics Letters,* Vol.91, p. 144107.
Qin, C.; Kozyrev, A. B.; Karbassi, A.; Joshkin, V. & van der Weide, D. W. (2007). *IEEE/MTT-S International Symp Dig.* P. 1145.
Qin, C. Kozyrev, A. B. Karbassi, A. & Van Der Weide, D. (2007) *Metamaterials*.
Scott, M. M.; Kostylev, M. P.; Kalinikos, B. A. & Patton, C. E. (2005). *Physical Review B,* Vol.71, p. 174440.
Seddon, N. & Bearpark, T. (2003). *Science,* Vol.302, p. 1537.
Service, R. F. (2003). *Science,* Vol.302, p. 1489.
Shadrivov, I. V. & Kivshar, Y. S. (2005). *Journal of Optics A: Pure and Applied Optics,* Vol.7, p. 68.
Shadrivov, I. V.; Morrison, S. K. & Kivshar, Y. S. (2006). *Optics Express,* Vol.14 .
Shadrivov, I.V.; Kozyrev, A.B.; van der Weide, D.W. & Kivshar, Yu.S. (2008). *Applied Physics Letters*, Vol.93, p. 161903.
Shadrivov, I.V.; Kozyrev, A.B.; van der Weide, D.W. & Kivshar, Yu.S. (2008). *Optics Express*, Vol.16, p. 20266.

Shalaev, V. M. (2007). *Nature Photonics,* Vol.1, p. 41.
Shelby, R. A.; D. R. Smith, D. R. & Schultz, S. (2001). *Science,* Vol.292, p. 77.
Sievenpiper, D. F. (2005). *IEEE Transactions on Antennas and Propagation,* Vol.53, p. 236.
Smith, D. R.; Padilla, W. J.; Vier, D. C.; Nemat-Nasser, S. C. & Schultz, S. (2000). *Physical Review Letters,* Vol.84, p. 4184.
Tien, P. K. (1958). *Journal of Applied Physics,* Vol.29, p.1347.
Tretyakov, S. A. (2001). *Microwave and Optical Technology Letters,* Vol.31, p. 163.
Veselago, V.G. (1968) *Soviet Physics Uspekhi, Vol.*10, p. 509.
Yagi, T. & Noguchi, A. (1976). *Electronics and Communications in Japan,* Vol.59, p. 1.
Yariv, A. (1988). *Quantum electronics*: Wiley.
Zharov, A. A.; Shadrivov, I. V. & Kivshar, Y. S. (2003). *Physical Review Letters,* Vol.91, p. 037401.

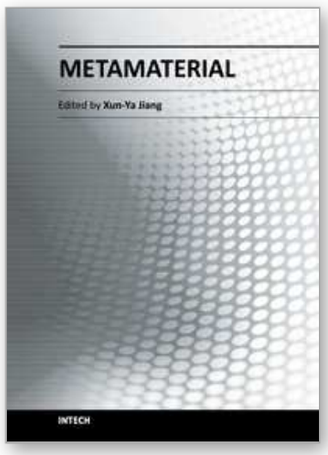

Metamaterial

Edited by Dr. Xun-Ya Jiang

ISBN 978-953-51-0591-6
Hard cover, 620 pages
Publisher InTech
Published online 16, May, 2012
Published in print edition May, 2012

In-depth analysis of the theory, properties and description of the most potential technological applications of metamaterials for the realization of novel devices such as subwavelength lenses, invisibility cloaks, dipole and reflector antennas, high frequency telecommunications, new designs of bandpass filters, absorbers and concentrators of EM waves etc. In order to create a new devices it is necessary to know the main electrodynamical characteristics of metamaterial structures on the basis of which the device is supposed to be created. The electromagnetic wave scattering surfaces built with metamaterials are primarily based on the ability of metamaterials to control the surrounded electromagnetic fields by varying their permeability and permittivity characteristics. The book covers some solutions for microwave wavelength scales as well as exploitation of nanoscale EM wavelength such as visible specter using recent advances of nanotechnology, for instance in the field of nanowires, nanopolymers, carbon nanotubes and graphene. Metamaterial is suitable for scholars from extremely large scientific domain and therefore given to engineers, scientists, graduates and other interested professionals from photonics to nanoscience and from material science to antenna engineering as a comprehensive reference on this artificial materials of tomorrow.

How to reference

In order to correctly reference this scholarly work, feel free to copy and paste the following:

Alexander B. Kozyrev and Daniel W. van der Weide (2012). Nonlinear Left-Handed Metamaterials, Metamaterial, Dr. Xun-Ya Jiang (Ed.), ISBN: 978-953-51-0591-6, InTech, Available from: http://www.intechopen.com/books/metamaterial/nonlinear-and-tunable-left-handed-metamaterials

INTECH
open science | open minds

InTech Europe
University Campus STeP Ri
Slavka Krautzeka 83/A
51000 Rijeka, Croatia
Phone: +385 (51) 770 447
Fax: +385 (51) 686 166
www.intechopen.com

InTech China
Unit 405, Office Block, Hotel Equatorial Shanghai
No.65, Yan An Road (West), Shanghai, 200040, China
中国上海市延安西路65号上海国际贵都大饭店办公楼405单元
Phone: +86-21-62489820
Fax: +86-21-62489821

IntechOpen